

Characterization and field-emission properties of carbon nanotube arrays in nanoporous alumina template and on blank Si substrate

Ching-Jung Yang, Chih Chen, and Jia-Min Shieh

Citation: [Journal of Applied Physics](#) **100**, 104302 (2006); doi: 10.1063/1.2375012

View online: <http://dx.doi.org/10.1063/1.2375012>

View Table of Contents: <http://scitation.aip.org/content/aip/journal/jap/100/10?ver=pdfcov>

Published by the [AIP Publishing](#)

Articles you may be interested in

[Field emission of large-area and graphitized carbon nanotube array on anodic aluminum oxide template](#)
J. Appl. Phys. **93**, 5602 (2003); 10.1063/1.1564882

[Field emission property of highly ordered monodispersed carbon nanotube arrays](#)
Appl. Phys. Lett. **78**, 3127 (2001); 10.1063/1.1372205

[Template-based carbon nanotubes and their application to a field emitter](#)
Appl. Phys. Lett. **78**, 2052 (2001); 10.1063/1.1359483

[In situ-grown carbon nanotube array with excellent field emission characteristics](#)
Appl. Phys. Lett. **76**, 3813 (2000); 10.1063/1.126790

[Controlling growth and field emission property of aligned carbon nanotubes on porous silicon substrates](#)
Appl. Phys. Lett. **75**, 481 (1999); 10.1063/1.124415



Re-register for Table of Content Alerts

Create a profile.



Sign up today!



Characterization and field-emission properties of carbon nanotube arrays in nanoporous alumina template and on blank Si substrate

Ching-Jung Yang and Chih Chen^{a)}

Department of Material Science and Engineering, National Chiao Tung University, Hsinchu, 30050 Taiwan, Republic of China

Jia-Min Shieh^{b)}

National Nano Device Laboratories, Hsinchu, 30078 Taiwan, Republic of China

(Received 9 March 2006; accepted 31 August 2006; published online 16 November 2006)

Ordered carbon nanotube (CNT) arrays were synthesized within anodized aluminum oxide template by thermal decomposition of hydrocarbon precursor with hydrogen ambient at growth temperature as low as 500 °C. Excess hydrogen in precursor mixture enables a steady supply of mobile hydrocarbon reactant which promotes facile solid-phase diffusion. The activation energy for CNT growth was determined to be 0.55 eV, a number smaller than 1.02 eV for similar precursor in nitrogen ambient. Moreover, CNTs grown in anodized aluminum oxide nanopores in this low temperature process were found to exhibit unusually high field-emission current of 100 mA/cm² at 8 V/μm. © 2006 American Institute of Physics. [DOI: 10.1063/1.2375012]

I. INTRODUCTION

One-dimensional (1D) carbon nanotubes (CNTs) have attracted many research groups in developing technologies and theories for nano-optoelectronic applications such as single-electron transistors,¹ field electron emitters,² and advanced interconnects.³ For the fabrication of practical CNT-based systems, one should identify a feasible method to grow dense and controllable CNT arrays in suitable substrate, preferably at moderate processing temperature. The nanotemplate method has been proposed to define distribution and morphology of the synthesized nanomaterials. Examples include self-assembled mesoporous silica (MS) matrix decorated with three-dimensional (3D) Si (Ge) nanocrystals⁴ and anodic aluminum oxide (AAO) embedded with two-dimensional (2D) CNT arrays.^{5,6} Typically, self-assembled template layers provide high aspect-ratio channels and interconnected nanopores that transportation of reactants is of critical concern. As the temperature is recognized to greatly affect diffusion process, the synthesis via nanotemplate approach is not known to occur at lower temperature than what would be allowed in bulk process.

Recently, many reports elucidate the synthesis of nanostructured materials at low temperature through a solid-phase diffusion (SPD) mechanism^{7–9} instead of the vapor-liquid-solid (VLS) growth mechanism.^{10,11} The observation of carbon nanofibers grown at room temperature is also reported.⁷ It is to be noted that enhanced precursor diffusivity due to plasma^{4,7,8} or hydrogen¹² was utilized to prepare crystalline films¹³ or nanostructures^{4,7–9} at significantly reduced growth temperature. Precursor with high mobility is expected to diffuse into the interiors of nanotemplates with less difficulty, but the plasma process is not suitable for applications that require substrates in large area. Therefore, thermal chemical vapor deposition (CVD) with hydrogen ambient could be a

promising technique for CNT growth on large-area substrate. Unfortunately, the deposition temperature for the thermal CVD process is around 550–900 °C,^{5,6} which is still too high for glass substrates to be used.

In this study, efficient field-emission CNT arrays on AAO template were fabricated by a thermal CVD method at 500 °C using a hydrocarbon precursor diluted with excess hydrogen. The activation energy for the CNT growth in C₂H₄/H₂ and C₂H₄/N₂ was determined with their respective growth mechanism discussed. This precursor mixture engenders the hydrogen-enhanced process that directly contributes to the reduction of growth temperature of CNTs. Field-emission characteristics of the CNT arrays were also measured for their potential application in display technology.

II. EXPERIMENT

To prepare the AAO on a Si substrate, sputtering of 20 nm TiN and 10 nm Ni was conducted successively onto a 4 in. (100) Si wafer. The TiN layer serves as a diffusion barrier to prevent silicidation of the Ni, which is required as the catalyst for subsequent CNT growth.¹⁴ Al film of 1.5 μm thickness was deposited on top of the Ni layer by thermal evaporation. Afterwards, the specimen was cut into pieces for AAO formation treatment. In anodization process, the specimen was mounted on a Teflon holder as anode and the cathode is a foil of platinum. Anodization was carried out in a 0.3M oxalic acid [(COOH)₂] aqueous solution at 25 °C under a constant voltage of 40 V for 30 min. The resulting irregular aluminum oxide film was immediately removed by dipping the specimen into a solution of 6 wt % phosphoric acid (H₃PO₄) and 1.8 wt % chromic acid (CrO₃) at 60 °C for 40 min. Then, a second anodization process was performed for 50 min with identical electrolyte composition and voltage like the first one. For both anodizations, the electrolyte was agitated using a magnetic stirrer for process uniformity. Finally, the AAO barrier layer at pore bottom was removed to expose the Ni catalytic layer. This was achieved

^{a)}Electronic mail: chih@cc.nctu.edu.tw

^{b)}Electronic mail: jmshieh@mail.ndl.org.tw

TABLE I. Experiment conditions for the growth of CNTs.

Sample	C ₂ H ₄ flow rate (SCCM)	H ₂ flow rate (SCCM)	N ₂ flow rate (SCCM)	H ₂ pretreatment (min)
A	125	500	0	10
B	125	0	500	10
C	50	200	0	10
D	50	0	200	10
E	125	50	0	10
F	125	0	50	10

through a pore widening treatment in 5 wt % phosphoric acid (H₃PO₄) solution for 30 min at 30 °C. For determination of activation energy for CNT growth as well as providing benchmark for electron emission characteristics, blank Si substrate with Ni/TiN (10 nm/20 nm) layers was used. The substrate underwent identical sputtering preparations as mentioned above.

A standard thermal CVD was employed to synthesize CNTs on AAO templated Si substrate and blank Si wafer. Prior to CVD process, both substrates were subjected to a reducing environment in a gas mixture of 75% hydrogen (H₂) and 25% nitrogen (N₂) at 500 °C for 15 min. Next, C₂H₄/H₂ or C₂H₄/N₂ was introduced in various ratios and flow rates at temperatures between 500 and 750 °C for 15 min to initiate CNT growth. Table I includes the processing parameters for the growth of CNTs in this work. The total flow rate was 625 SCCM (SCCM denotes cubic centimeter per minute at STP). The schematic of the entire fabrication process is shown in Fig. 1. The AAO templates and the CNTs were examined by JEOL JSM-6500F field-emission scanning electron microscopy (FE-SEM). Field-emission measurements were conducted by a simple diode configuration in high vacuum chamber of 10⁻⁶ torr. A tungsten probe with a diameter of 500 μm was used as the anode. The distance between the CNT array (as cathode) and the anode was controlled by a precise screw meter and was kept at 100 μm for our experiment. The CNT array was biased with a positive voltage from 0 to 1000 V at room temperature to extract electrons. A high voltage source unit (Keithley 237) was used for providing the sweeping electric field (*E*) and monitoring the emission current density (*J*). Prior to the field-emission measurement, a high voltage of 600 V was applied to the CNT array to oxidize undesirable adsorbed molecules.

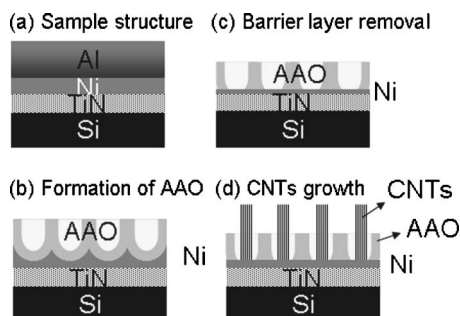


FIG. 1. Schematic diagram for the fabrication process of CNTs on an AAO template.

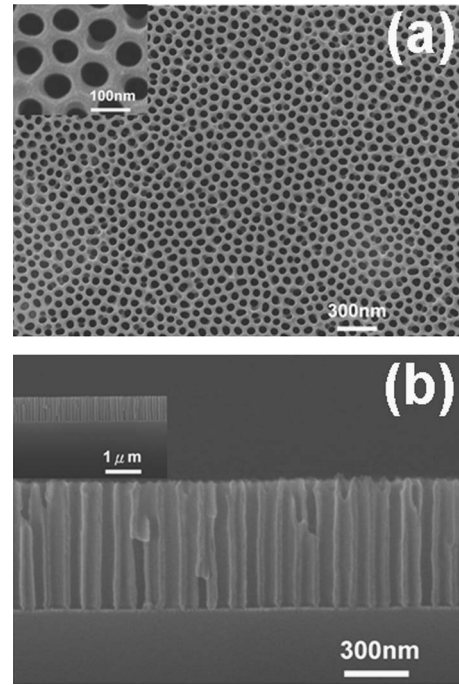


FIG. 2. (a) Top-view and (b): cross-sectional SEM images of AAO template fabricated on a Si substrate.

III. RESULTS AND DISCUSSION

Figures 2(a) and 2(b) show the top-view and cross-sectional SEM images of the as-synthesized AAO before the CNT growth. Ordered pore channel arrays with pore size of 75 nm and pore-to-pore distance of 100 nm was observed on the substrates following the two-step anodization.¹⁵ The aspect ratio for the AAO channels is about 10. Figures 3(a) and 3(b) show the morphology of the CNTs on the AAO template using recipe A in Table I. Initially, relatively few CNTs were observed in the pores of the AAO template with negligible entanglement among them. After 15 min of growth time, dense CNTs were present and its density (the ratio of filled pores) was estimated to be of 2.2×10^9 tubes/cm² ($\sim 28\%$). Figure 4 shows a typical morphology for the CNTs grown on the blank Si wafer at 500 °C for 15 min. Although the growth conditions were identical for both Figs. 3 and 4, the morphology of the CNTs grown on the blank Si substrate demonstrated substantial entanglements with density estimated at 6.5×10^{10} tubes/cm².

The field-emission characteristics of the CNTs arrays on both substrates were examined with their results shown in Fig. 5. For AAO templated Si substrate, the electron emission current density was found to attain 100 mA/cm² under an electric field of 8 V/μm. In addition, the turn-on field, the electric field when the emission current density reaches 10 μA/cm², was 2.8 V/μm. In contrast, the electron emission current density was merely 10 mA/cm² at the same electric field for blank Si wafer and its turn-on field was 4.5 V/μm. The plotting of $\ln(I/V^2)$ vs $1/V$, as shown in the inset of Fig. 5, could extract the slope. Following Fowler-Nordheim¹⁶ (FN) relation, the field enhancement factor β were 2700 for AAO templated Si substrate whereas it was only 505 for blank Si wafer. This β factor of 2700 was

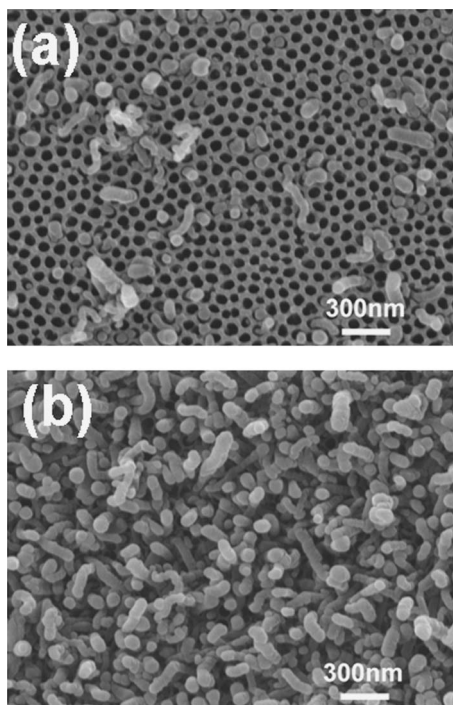


FIG. 3. Top-view SEM images showing CNTs growth on AAO layers after (a) 10 min and (b) 15 min by a thermal CVD method at the temperature of 500 °C using the recipe A in Table I.

the highest reported to date.^{5,6,17–19} Chen *et al.* also reported a similar field-emission current density with slightly higher CNT density of $(6–8) \times 10^9$ tubes/cm² using AAO as a template for CNT growth.¹⁸ Low screening effect among individual CNTs is likely to be responsible for the enhanced field-emission properties in this study. As clearly seen in Fig. 3, the filling ration of the CNTs was 28% and physical entanglements among them were minimized by AAO template.

The field-emission properties for the CNTs arrays prepared by our approach are comparable to those obtained from CNTs derived from plasma enhanced growth. However, they are significantly better than those obtained by thermal CVD with precursor mixture in low hydrogen content, as listed on Table II. The uniqueness of our process enables us to grow CNTs at temperature as low as 500 °C without the assistance of plasma. Although other types of quasi-one-dimensional objects such as carbon nanofibers (CNFs) were synthesized at certain low temperatures^{10,11,20} or even at

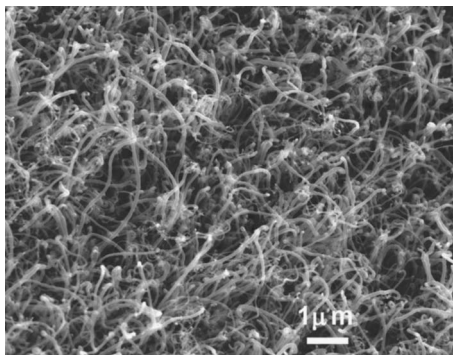


FIG. 4. Plan-view SEM image for the CNTs morphology grown on the blank Si wafer at 500 °C for 15 min.

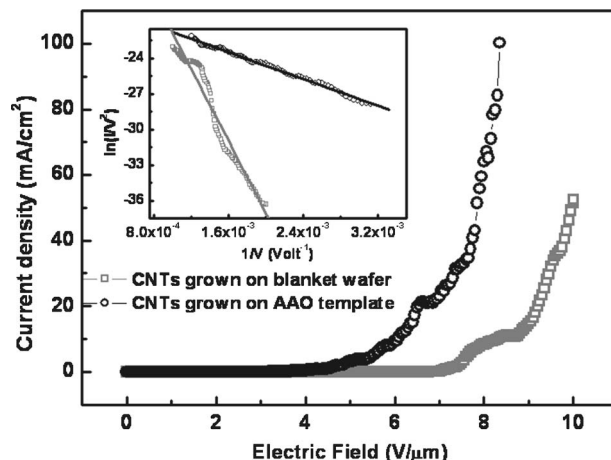


FIG. 5. Field-emission characteristics of CNTs grown on AAO template and on blank wafers by a thermal CVD method using the recipe A in Table I. The inset shows FN plots for two curves shown on this figure.

room temperature,⁷ their implementation especially for display application is uncertain as field-emission efficiency data are lacking.

The VLS mechanism is often used to describe the catalytic growth of CNTs.^{9,11,21,22} The synthesis process should provide sufficient energy to produce molten catalytic particles for subsequent alloying with impinging gaseous reactants. Carbon segregation at the bottom of the particle results in a stable graphitic structure.²³ As indicated, the minimum growth temperature for CNT formation in VLS model is given by the eutectic temperature of carbon and catalyst element. Previous studies on SPD (Refs. 7–9) process involved catalytic synthesis of nanostructures such as CNFs,^{7,8} ZnSe,¹⁰ and GaAs (Ref. 9) nanowires (NWs) at relatively low temperature. It was suggested that plasma^{7,8} and molecular-beam epitaxy¹⁰ (MBE) techniques were conducive to facile diffusion of adsorbed reactants along the surface of catalyst particles. Generally, plasma is known to dissociate precursors,⁸ etch materials in amorphous phase on reacting surfaces,⁷ as well as promote the diffusion capability of the reactive species.^{8,9} These processes are recognized to benefit the SPD process.^{7–10} For example, Kamins *et al.*²⁴ announced Ti-promoted Si NW growth at temperatures below the Si–Ti eutectic point by CVD method using the feed of excess precursors. In this study, the growth temperature was far below the C–Ni eutectic point of 1311 °C.⁸ Thus the growth mechanism is of particular interest. Previously, it was suggested that plasma heating and dissociative adsorption of hydrocarbon molecules would engender localized heating near the surface of the catalyst and cause surface melting at reduced growth temperature.²⁵ Therefore, the VLS model may still be valid for our growth conditions. On the other hand, it is likely that SPD process might contribute to some degrees. However, the exact growth mechanism is not clear at this moment, and further study is necessary.

In our study, both the total flow rate and hydrogen ratio for the reacting precursor mixture are two to three times larger than those reported in other works.^{11,20–22} Such a mixture not only allows for a steady supply of carbon atoms at the surface of the Ni particle but also promotes the dissocia-

TABLE II. Comparison of field-emission characteristics and parameters for CNT growth by our approach with those obtained by other research groups.

		Temperature (°C)	Dilution gas	Field emission	Reference
Thermal CVD	on AAO	550–900	Ar < 160 SCCM H ₂ < 40 SCCM N ₂ < 100 SCCM NH ₃ < 60 SCCM	$\beta = 80\text{--}5600$ Current density 24 mA/cm ²	5 and 6
	On blank	700–800	Ar < 60 SCCM H ₂ < 200 SCCM N ₂ < 60 SCCM NH ₃ < 300 SCCM He < 15 SCCM	$\beta = 800\text{--}7800$ Current density 100 mA/cm ²	15 and 17
Plasma technique CVD	On AAO	600–660	H ₂ = 2–80 SCCM	$\beta = 1900\text{--}2600$ Current density 100 mA/cm ²	18
	On blank	280–700	H ₂ = 2–270 SCCM CO ₂ < 30 SCCM N ₂ = 2–100 SCCM	$\beta = 3000$ Current density 173 mA/cm ²	19 and 27 19 and 27
Our work	on AAO	500	H ₂ = 500 SCCM	$\beta = 2700$ Current density 100 mA/cm ²	

tion of hydrocarbon reactants.²² Moreover, high hydrogen content enhances surface self-diffusion,²⁶ and removes amorphous materials by hydrogen etching.²⁴ These proposed effects in our approach can be examined by varying the growth rate with temperature as performed before by Hofmann *et al.*^{11,20} Figures 6(a)–6(f) show the cross-sectional SEM images for the CNTs on blank Si substrate with the hydrogen flow for 15 min at 500, 550, 600, 650, 700, and 750 °C, respectively. The length of the CNTs increases as the growth

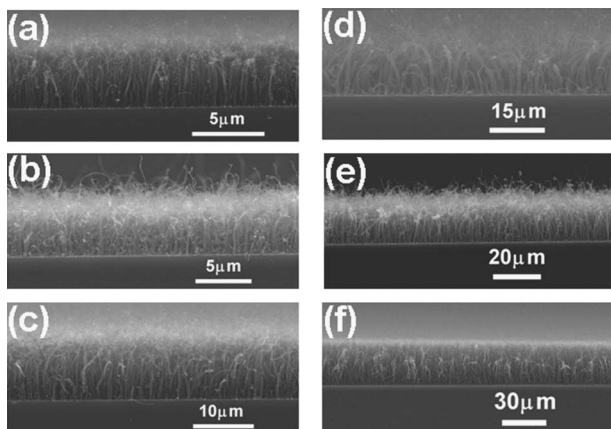


FIG. 6. Cross-sectional SEM images showing the CNTs grown on the blank Si substrate for 15 min at various temperatures: (a) 500 °C, (b) 550 °C, (c) 600 °C, (d) 650 °C, (e) 700 °C, and (f) 750 °C.

temperature was raised. Figure 7 compares the growth rate of the CNTs at 650 °C for our samples A–F and the sample of Ducati *et al.*²² The growth conditions are listed in Table I. The growth rate of the CNTs grown on the blank Si substrate was about 18 nm/s which is much higher than one obtained for thermal CVD (3.5 nm/s).²² Base on the Arrhenius plot of growth rate versus reciprocal growth temperature ($1/T$) as

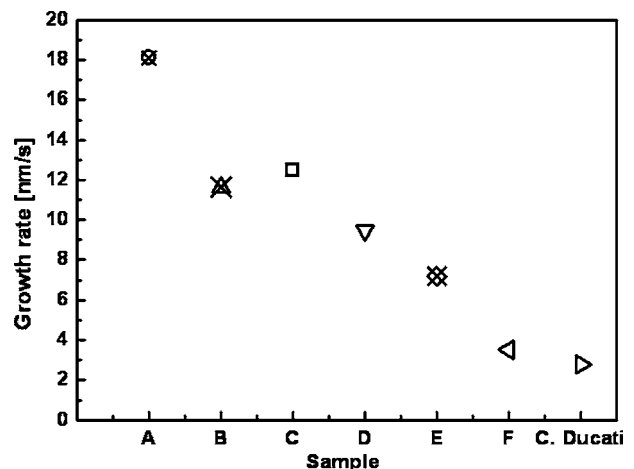


FIG. 7. Growth rate of CNTs on blank Si wafer by thermal CVD method at 650 °C using various recipes listed on Table I. For comparison, the growth rate for CNTs grown by CVD with conventional recipes reported by Ducati *et al.* was also shown.

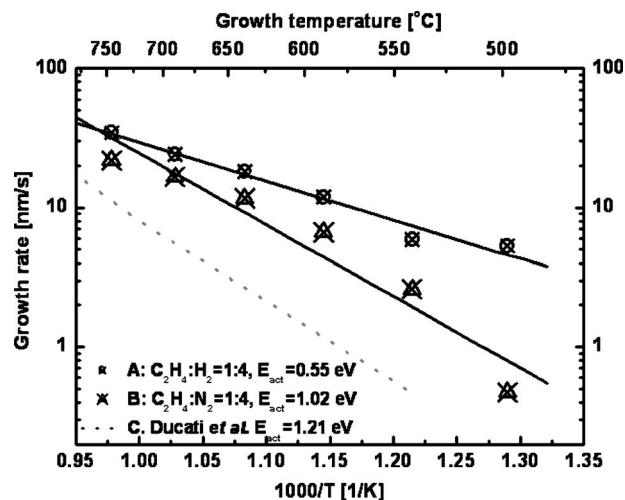


FIG. 8. Arrhenius plot of growth rate vs reciprocal growth temperature ($1/T$) for high hydrogen (nitrogen)-diluted recipes. For comparison, the plot for CNTs grown by CVD with conventional recipes reported by Ducati *et al.* was also shown.

shown in Fig. 8, activation energy E_A for our case with precursor with high hydrogen content was determined to be 0.55 eV. This value is slightly higher than 0.23 eV from the plasma synthesis route but much lower than 1.21 eV derived from standard thermal CVD.^{11,21} When hydrogen dilution was replaced with nitrogen dilution, the growth rate was reduced by two times and the activation energy was increased to 1.02 eV. Decreasing either the total flow rate or hydrogen (nitrogen) dilution also reduce the growth rate, as shown in Fig. 7. Therefore we conclude that excess hydrogen dilution and abundant precursor inflow would initiate CNT growth at faster rate with possibly lower activation energy. As a result, we observe the CNT growth at relatively low temperature.

It is known that the growth rate of CNTs is nonlinear with respect to the growth duration. Evidence indicates that the growth rate tend to saturate after first 10–20 min. To verify whether our growth rates were obtained before or after saturation, we measured the growth rates after 10 min using other sets of samples. Table III(a) summarizes the height of CNTs and corresponding growth rates for both 10 and 15 min growth time for $C_2H_4:H_2=1:4$. We found that the growth rate measured at 15 min was faster than that measured at 10 min, which indicates growth saturation was not attained after 15 min. The activation energy derived from the data measured at 10 min was 0.57 eV, which is close to 0.55 eV obtained at 15 min. Similarly for $C_2H_4:N_2=1:4$, no saturation on growth rate was observed up to 15 min as shown in Table III(b). The activation energy obtained from the data at 10 min was 1.08 eV, which is quite close to 1.02 eV obtained at 15 min. Therefore, the activation energy we obtained using the data at 15 min should be reliable.

It is especially noted that we expect high hydrogen-diluted flow also enhances the transportation of reactants into the nanopores of the AAO template and the removal of amorphous carbon on the top surfaces of the AAO template. In addition, it was reported that the AAO nanopores would promote CNT growth.¹⁴ Therefore, the quality of CNTs was

TABLE III. The height of CNTs and the corresponding growth rates measured at 10 and 15 min. (a) $C_2H_4:H_2=1:4$ and (b) $C_2H_4:N_2=1:4$.

Growth Temp. (°C)	Growth time: 10 min		Growth time: 15 min	
	CNT height (nm)	Growth rate (nm/s)	CNT height (nm)	Growth rate (nm/s)
(a)				
500	1 980	3.3	4 780	5.31
550	3 150	5.25	5 300	5.89
600	5 350	8.92	10 700	11.89
650	8 150	13.58	16 300	18.11
700	10 868	18.11	21 735	24.15
750	15 546	25.91	31 090	34.54
(b)				
500	213	0.35	426	0.47
550	750	1.25	2 330	2.59
600	1 580	2.63	6 010	6.68
650	3 550	5.92	10 470	11.63
700	6 270	10.45	14 980	16.64
750	11 950	19.92	19 680	21.87

further improved when they were grown on the AAO template even at a low temperature, a result suggested in Figs. 2 and 3.

IV. CONCLUSIONS

In conclusion, efficient field-emission CNT arrays on the AAO templated Si substrate was prepared at temperature as low as 500 °C by a CVD method with hydrocarbon precursor in high hydrogen ambient. This approach enables sufficient reactants with high diffusivity, promotes dissociation of hydrocarbon reactants, as well as facilitates etching of amorphous carbon by-products. Field-emission current density of 100 mA/cm² at 8 V/μm was measured. In addition, the activation energy for the CNT growth was determined to be 0.55 eV. We believe that high hydrogen content is beneficial to the VLS and SPD processes, which leads to relatively reduced growth temperature.

¹C. Thelander, T. Mårtensson, M. T. Björk, B. J. Ohlsson, M. W. Larsson, L. R. Wallenberg, and L. Samuelson, *Appl. Phys. Lett.* **83**, 2052 (2003).

²N. G. Shang, F. Y. Meng, F. C. K. Au, Q. Li, C. S. Lee, I. Bello, and S. T. Lee, *Adv. Mater. (Weinheim, Ger.)* **14**, 1308 (2002).

³Y. Xia *et al.*, *Adv. Mater. (Weinheim, Ger.)* **15**, 353 (2003).

⁴A. T. Cho *et al.*, *Electrochem. Solid-State Lett.* **8**, G143 (2005).

⁵H. Gao *et al.*, *J. Appl. Phys.* **93**, 5602 (2003).

⁶S. M. Yoon, J. Chae, and J. S. Suh, *Appl. Phys. Lett.* **84**, 825 (2004).

⁷T. M. Minea, S. Point, A. Granier, and M. Touzeau, *Appl. Phys. Lett.* **85**, 1244 (2004).

⁸B. O. Boskovic, V. Stolojan, R. U. A. Khan, S. Haq, and S. R. P. Silva, *Nat. Mater.* **1**, 165 (2002).

⁹A. I. Persson, M. W. Larsson, S. Stenström, B. J. Ohlsson, L. Samuelson, and L. R. Wallenberg, *Nat. Mater.* **3**, 677 (2004).

¹⁰A. Colli *et al.*, *Appl. Phys. Lett.* **86**, 153103 (2005).

¹¹S. Hofmann, C. Ducati, J. Robertson, and B. Kleinsorge, *Appl. Phys. Lett.* **83**, 135 (2003).

¹²S. Sriraman, S. Agarwal, E. S. Aydil, and D. Maroudas, *Nature (London)* **418**, 62 (2002).

¹³J. H. Wu, J. M. Shieh, B. T. Dai, and Y. C. S. Wu, *Electrochem. Solid-State Lett.* **7**, G128 (2004).

¹⁴A. M. Rao, D. Jacques, R. C. Haddon, W. Zhu, C. Bower, and S. Jin, *Appl. Phys. Lett.* **76**, 3813 (2000).

¹⁵E. J. Bae, W. B. Choi, K. S. Jeong, J. U. Chu, G. S. Park, S. Song, and I. K. Yoo, *Adv. Mater. (Weinheim, Ger.)* **14**, 277 (2002).

- ¹⁶R. H. Fowler and L. W. Nordheim, Proc. R. Soc. London, Ser. A **119**, 173 (1928).
- ¹⁷S. Wei, W. P. Kang, W. H. Hofmeister, J. L. Davidson, Y. M. Wong, and J. H. Hung, J. Vac. Sci. Technol. B **23**, 793 (2005).
- ¹⁸P. L. Chen, J. K. Chang, C. T. Kuo, and F. M. Pan, Diamond Relat. Mater. **13**, 1949 (2004).
- ¹⁹C. F. Chen, C. L. Lin, and C. M. Wang, Thin Solid Films **444**, 64 (2003).
- ²⁰S. Hofmann, C. Ducati, B. Kleinsorge, and J. Robertson, Appl. Phys. Lett. **83**, 4661 (2003).
- ²¹S. Hofmann, G. Csányi, A. C. Ferrari, M. C. Payne, and J. Robertson, Phys. Rev. Lett. **95**, 036101 (2005).
- ²²C. Ducati, I. Alexandrou, M. Chhowalla, G. A. J. Amaratunga, and J. Robertson, Appl. Phys. Lett. **92**, 3299 (2002).
- ²³A. V. Melechko, V. I. Merkulov, T. E. Mcknight, M. A. Guillorn, K. L. Klein, D. H. Lowndes, and M. L. Simpson, J. Appl. Phys. **97**, 041301 (2005).
- ²⁴T. I. Kamins, R. S. Williams, D. P. Basile, T. Hesjedal, and J. S. Harris, J. Appl. Phys. **89**, 1008 (2001).
- ²⁵V. Kayastha, Y. K. Yap, S. Dimovski, and Y. Gogotsi, Appl. Phys. Lett. **85**, 3265 (2004).
- ²⁶S. Horch, H. T. Lorensen, S. Helveg, E. Lægsgaard, I. Stensgaard, K. W. Jacobsen, J. K. Nørskov, and F. Besenbacher, Nature (London) **398**, 134 (1999).
- ²⁷W. H. Wang, Y. T. Lin, and C. T. Kuo, Diamond Relat. Mater. **14**, 907 (2005).